Thampy *et al.*
Journal of Engineering and Applied Science (2023) 70:111
https://doi.org/10.1186/s44147-023-00261-1

Journal of Engineering and Applied Science

RESEARCH Open Access

Inline induction heating for high-pressure fuel-based testing applications

Tom Thampy[1], Emmanuel Gospel Raj Rivington[1*], Madan Mohan Avulapati[2] and Niroop Srinivasa Murthy[1]

*Correspondence: empelraj@gmail.com

[1] Aerospace Systems, Central Manufacturing Technology Institute, Bengaluru, Karnataka, India
[2] Department of Mechanical Engineering, Indian Institute of Technology Tirupati, Tirupati, Andhra Pradesh, India

Abstract

Induction heating offers numerous advantages over conventional methods for heating high-pressure fluids in hydraulic testing applications. It simplifies complex processes, mitigates the risks associated with high-pressure environments, and enhances overall safety. The design of an efficient induction heating system requires a clear understanding of its key components, including the resonant tank circuit, impedance matching and isolation stage, high-frequency inverter, driver circuitry, and controller. The configuration of the resonant circuit plays a crucial role in device ratings and control methods. To meet the demanding requirements of switching devices like IGBTs, the driver circuit must ensure high immunity to interferences and failure. Effective system design allows the heating circuit to operate close to resonant switching, minimizing switching losses and cooling requirements. This paper presents the design and development of a 4-kW induction heater specifically tailored for inline heating of aviation fuel under high pressure. The system aims to achieve a precise temperature profile for testing line-replaceable units (LRUs) used in aircraft. The design methodology encompasses the selection of the resonant tank circuit configuration, impedance matching and isolation stage, high-frequency inverter, driver circuitry, and control strategies. Through extensive simulations in LTspice and experimental measurements, power losses in different components of the power conversion circuits are assessed, and overall system efficiency is evaluated. The results demonstrate the proposed induction heating system's remarkable energy efficiency, reduced switching losses, and improved reliability. Furthermore, a comprehensive comparison with existing designs and industry norms is presented, highlighting the distinct advantages of the proposed system in terms of cost-effectiveness, energy efficiency, material utilization, and processing time. This research contributes valuable insights into the design and optimization of induction heating systems for high-pressure fluid heating applications, providing a practical and efficient solution for the aviation industry.

Keywords: Inline induction heating, Resonant inverters, Closed-loop systems

Introduction

High-temperature testing is a crucial requirement for qualifying aircraft engine system hydraulic line-replaceable units (LRUs), including servo valves, actuators, filters, and more. These components often operate with aviation fuel as the working fluid and undergo testing with aviation fuel at high pressures, following specific temperature

profiles as illustrated in Fig. 1. These temperature profiles aim to simulate the operational conditions and endurance of the aircraft over several flight hours.

Inline heating of the fuel is a preferred approach to ensure a continuous supply of dynamically heated fuel while minimizing energy expenses and the need for hot reservoirs. However, achieving the required temperature profiles through heating fuel at high pressures presents several challenges. Traditional immersion heating elements cannot withstand the high pressures inside the hydraulic lines, and their rupture within the system would pose significant safety hazards.

In contrast, induction heating emerges as a superior choice due to its non-invasive nature, electrical isolation, cleanliness, and several advantageous features such as flexibility, controllability, fast heating, repeatability, and safety [1–5]. This paper focuses on elaborating the design approach of a 4-kW induction heater specifically developed for inline heating of aviation fuel at a pressure of 84 bar and a flow rate of 1 lpm, incorporating closed-loop control.

The system's basic block diagram, as depicted in Fig. 2, illustrates the interaction between the main process controller, the PID controller responsible for temperature regulation, and the induction heater, which is controlled using an ON/OFF strategy.

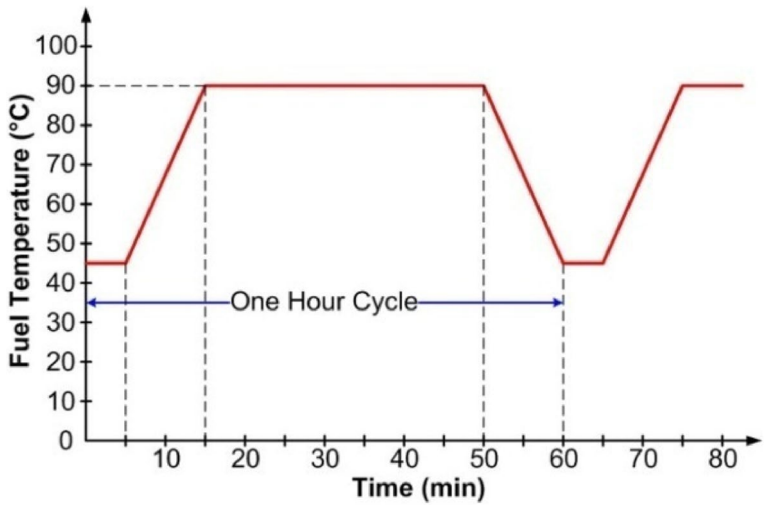

Fig. 1 Typical fuel temperature profile for testing aircraft engine system hydraulic LRUs

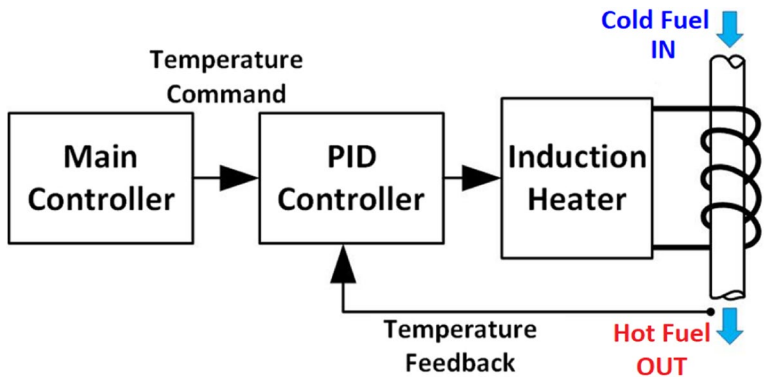

Fig. 2 Overall scheme of induction heating control with temperature feedback

The command signals to the PID controller are suitably adjusted to achieve the temperature profile shown in Fig. 1.

Methods

Induction heating technique is widely used in numerous low- to high-power applications due to the various advantages it offers. The basic approach in the implementation of an induction heating system involves producing high-frequency alternating magnetic flux to generate heat in a conductive workpiece through the eddy currents induced in the workpiece. The technique utilizes the skin effect that forces the current to be concentrated near the surface of the object, thereby increasing the effective resistance of the workpiece producing more heat [6]. The thickness of this region where the current gets concentrated or the skin depth is given by [1, 2]

$$\delta = \sqrt{\frac{2\rho}{2\pi f \mu}}(m) \tag{1}$$

where

ρ is electrical resistivity (Ω m)

f is the frequency (Hz)

μ is the magnetic permeability (H/m)

Heat pipe

In the case of a solid workpiece made of steel, the heat generated near the outer surface of the workpiece gets conducted to the inner portion of the workpiece to make it uniformly hot. However, during active heating through the induction technique, there exists a temperature gradient from the outer surface of the workpiece to its center due to the low specific heat capacity of the steel resulting in slow heat transfer. Instead, if the workpiece is a steel pipe with a thickness comparable with the skin depth, and carries a liquid with high specific heat capacity, such as aviation fuel, or even water, the heat produced near the surface of the workpiece can easily get conducted to the liquid inside, making it hot.

The heating pipe should however be sufficiently long to prevent excessive heating power focused on a small surface area of the heating pipe and causing rupture at high pressure due to heat.

The heating arrangement comprises a low carbon steel pipe with a 22-mm outer diameter and 2 mm thickness, which acts as the workpiece and is surrounded by a 19-turn helical copper coil with a pipe diameter of 8 mm and wall thickness of 2 mm. The length of the steel pipe under the coil is around 450 mm. As the copper coil is excited with a high-frequency alternating current, heat is induced through eddy currents near the outer surface of the pipe which is conducted across the thickness of the pipe and then transferred to the fuel that is passing through the pipe. Figure 3 shows the simulated view of this arrangement with a power input of 4 kW fed for a period of 5 s.

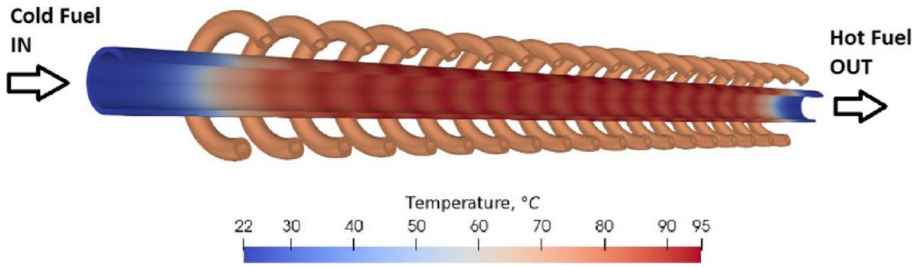

Fig. 3 Simulated view of the induction heated 22 mm dia steel pipe for inline fuel heating application with CENOS

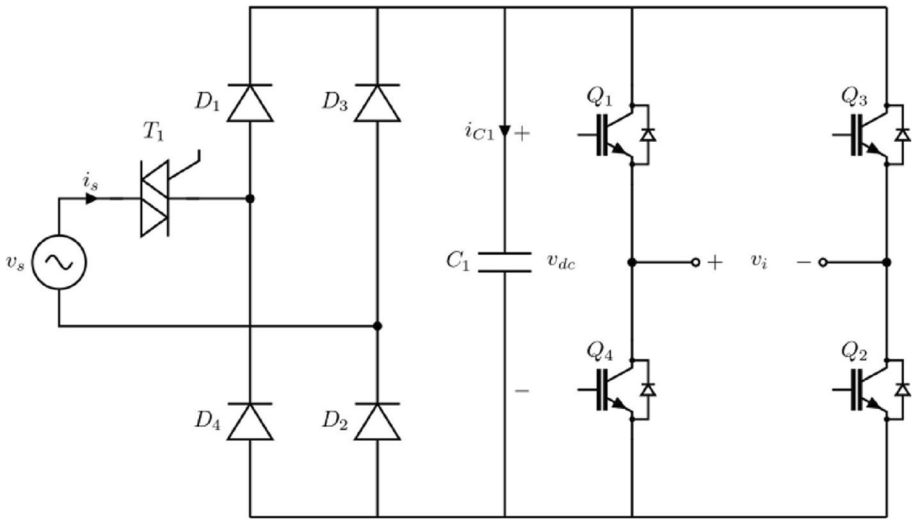

Fig. 4 Power circuit of the induction heater with AC power supply, AC voltage controller, bridge rectifier, and high-frequency inverter

Power circuit

The power circuit for the induction heater comprises of a high-frequency inverter as shown in Fig. 4 [7]. The DC voltage input to the inverter is obtained from a single-phase AC power supply through an AC voltage controller T_1 and a bridge rectifier. The inverter is operated at a constant frequency, while the AC voltage controller is used for implementing the closed-loop PID control.

Capacitor C_1 is required to absorb the reactive currents from the output of the inverter without allowing high ripple voltages in the DC link [8]. However, as the induction heating inverter operates at high frequency and at resonance, with almost negligible reactive currents, a low DC link capacitance is usually sufficient.

The value of capacitance is calculated from the basic capacitor equation

$$i_{c_1} = C_1 \frac{dv_{c_1}}{dt} \tag{2}$$

where i_{c_1} is the change in current (A),

C_1 is the capacitance (F),

dv_{c_1} is the change in capacitor voltage (V), and

dt is the change in time (s).

Rearranging (2),

$$C_1 = \frac{i_{c_1}}{2fdv_{c_1}} \tag{3}$$

where f is the frequency (Hz).

Considering the peak ripple current as 10 percent of 15 A load current and 2 V as allowable ripple voltage at the DC link when operating at 37 kHz frequency, the DC link capacitance is given by

$$C_1 = \frac{1.5}{2 \times 37 \times 10^3 \times 2} = 10.1\mu F$$

Polymer capacitor bank of 12 µFis used for the DC link due to its fast dynamic response and durability. IGBTs are ideal as switching devices for high-power resonant switching applications such as induction heating. They are capable of handling large power levels with low power gate drive [1, 7]. The IGBTs Q_1, Q_2, Q_3, and Q_4 are essentially fast-switching devices capable of operating till 100 kHz [7]. Their switching losses increase considerably beyond the frequency of 50 kHz with non-zero switching, which may prove to be highly inefficient. The IGBTs should be rated for at least 400 V, considering the peak voltage of 325 V DC link voltage at no load and possible overvoltages due to reactive currents from the load. Current rating of the IGBTs should be at least 5 to 7 times higher than the maximum instantaneous operating current to accommodate switching losses during non-zero switching conditions [9, 10]. 600 V, 100 A fast switching IGBTs are used as switching devices in the given application to enable high-frequency switching. A 2 µs dead time is maintained between the switching of IGBTs to allow safe turn-off and to prevent shoot-through of the inverter legs.

Resonant circuit — parallel LC

Induction heating requires high-frequency flux produced by the heating coil to be linked with the workpiece to produce induced currents in the workpiece with an enhanced skin effect. Producing high-frequency flux requires high-frequency current flowing in the heating coil. It is generally difficult to establish high-frequency currents in a coil due to the high inductive reactance naturally exhibited by the coil. Establishing resonance between the inductance of the heating coil and the capacitance of a suitable tank capacitor helps cancel the inductive behavior of the heating coil, enabling easy passage for high-frequency currents through the heating coil.

The resonant circuit for an induction heater could be based on either a parallel LC circuit or a series LC circuit. Figure 5 shows the typical schematic of a parallel resonant induction heating circuit with a capacitor bank C_2 connected in parallel with the heating coil with reactance X_L. Resistance of the steel pipe to be heated R_L is reflected on the heating coil in such a way that the effective impedance of the heating coil becomes $R_L^{'} + jX_L$ [1]. Parallel resonant induction heating circuits require the usage of impedance matching/filter inductor L_m or a current source inverter for enabling efficient power delivery to the heating load [7]. Power delivered to the heating

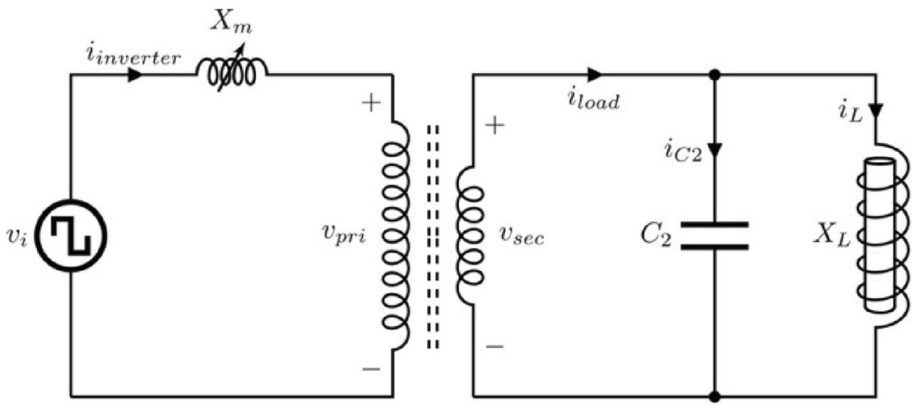

Fig. 5 Parallel resonant isolated heating circuit

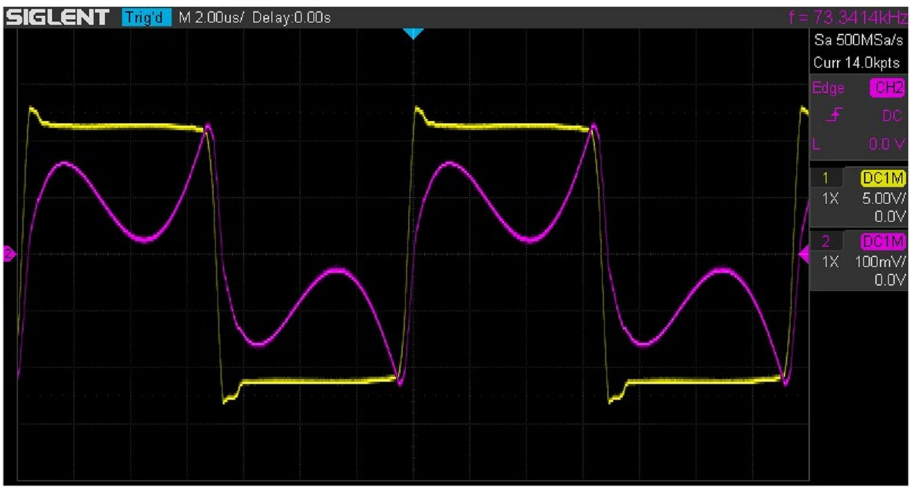

Fig. 6 Inverter output voltage (yellow) and current (pink) of parallel resonant induction heater

load could also be controlled to some extent by adjusting the reactance value X_m of the impedance matching inductor, although this method of power control is not recommended.

The inverter output voltage and the current for a parallel resonant induction heater are shown in Fig. 6. The main drawback of the parallel resonant induction heater is that even though the tank circuit current or the individual currents through the heating coil or capacitor is sinusoidal, the inverter current is non-sinusoidal due to suppression from the tank circuit near peaks of each cycle, which makes it difficult to transfer power from the inverter to the tank circuit for effective heating of the workpiece. Moreover, the parallel resonant induction heating circuit must operate exactly at its resonant frequency to keep the inverter current minimum. Frequencies higher than the resonant frequency increase the inductive reactance of the heating coil decreasing the coil current and the heat produced on the workpiece, on the other hand, decreases the capacitive reactance, causing an increase in capacitor current, which is undesirable. Frequencies lower than the resonant frequency cause reduction in skin effect, drawing higher currents from the inverter for the same heat produced.

Fig. 7 Inverter voltage (yellow) and current (pink) of a parallel resonant induction heater with low matching inductor

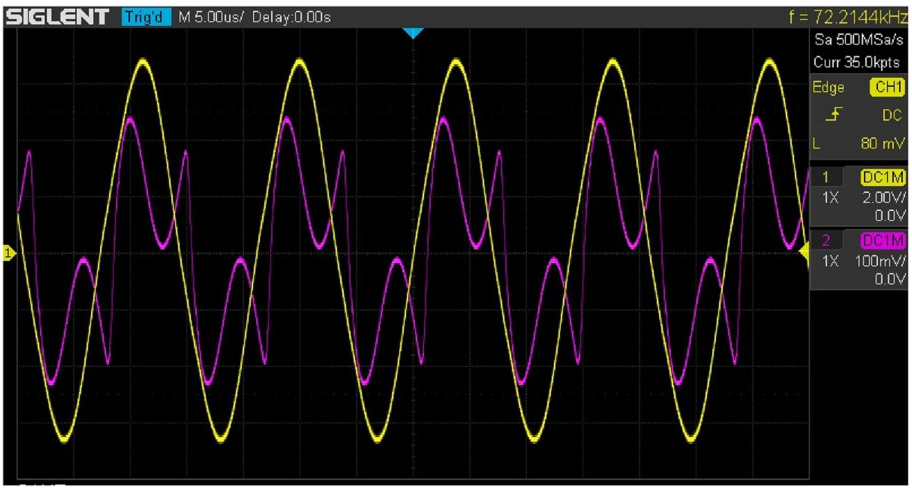

Fig. 8 Resonant current (yellow) and inverter current (pink) of parallel resonant induction heater

With low values of matching inductor X_m, the inverter current becomes increasingly reactive despite the inverter operating at resonant frequency due to the rejecting behavior of the parallel resonant tank circuit [6]. The inverter current becomes almost fully reactive as shown in Fig. 7 when X_m is close to zero. It can be observed that there is a change in inverter voltage within half cycles due to the high reactive currents charging and discharging the DC link.

Figure 8 shows how the inverter current is shaped by the influence of the sinusoidal voltage of the parallel resonant tank circuit and the inverter switching. The graph showing the inverter current and IGBT gate pulses for the best-adjusted impedance matching inductor is shown in Fig. 9. Higher value of the matching inductor would reduce the amplitude of the inverter current, reducing the output power.

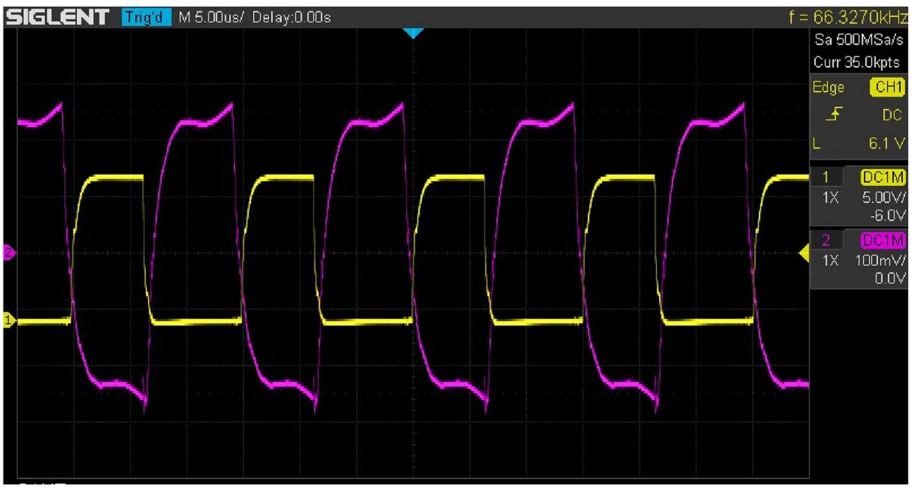

Fig. 9 IGBT gate voltage (yellow) and inverter current (pink) of a parallel resonant induction heater with high matching inductor

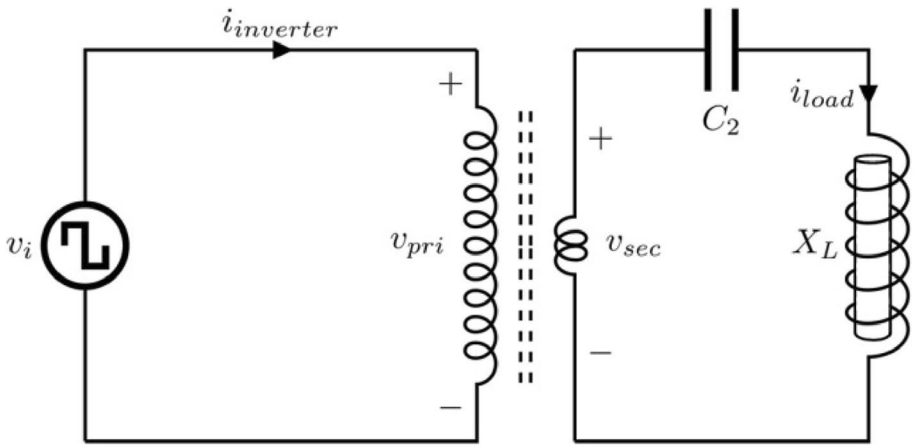

Fig. 10 Series resonant isolated heating circuit with secondary side resonant capacitor

Resonant circuit — series LC

The resonant circuit can also be designed with the resonant capacitor C_2 in series with the heating coil X_L as shown in Fig. 10. The significant advantage of a series resonant circuit for induction heater is that it readily accepts power from the inverter without the need of a matching inductor as in the parallel resonant induction heating circuit [11–13]. Unlike the parallel resonant induction heater circuit, the inverter operation in a series resonant induction heater can be safely deviated away from resonance frequency with the inverter current reducing. However, the inverter is always controlled "above-resonance" to prevent capacitive switching at frequencies lower than resonant frequency [14].

The secondary circuit carries large resonant currents that flow through the heating coil. It is therefore important that the tank capacitor C_2 and the secondary winding of the transformer are rated for such high current values. The transformer is designed with a ratio of 1:12. Small voltages are usually sufficient to drive a series resonant

circuit as the resonant voltages across the heating coil and the capacitor C_2 are in phase opposition with each other. The resonant current in the tuned secondary circuit being naturally sinusoidal [2], forces the inverter current on the primary side also to be sinusoidal in shape as shown in Fig. 11. This enables resonant switching in the inverter side and results in low switching loss at resonance [1, 2, 10].

The capacitance required could be calculated from the expression of resonant frequency as [8]

$$f_r = \frac{1}{2\pi}\sqrt{LC_2} \tag{4}$$

The choice of resonant frequency is based on factors such as the type of switching device, material to be heated, and audio frequency range. Ultrafast IGBTs are suitable for switching frequencies up to 100 kHz. However, the frequency should be kept as low as possible to minimize the switching losses. If the electrical resistance of the material to be heated is low, the operating frequency needs to be increased sufficiently high to decrease the skin depth and increase the resistance. This is the reason why heating aluminum or copper requires frequencies from 100 kHz to over 1 MHz. Keeping the resonant frequency below 20 kHz may create audible noise from the system [8]. Based on the above understanding, the operating frequency is selected as 33 kHz.

With a desired resonant frequency of 33 kHz given the inductance of the heating coil 1. 94 μH,

$$\begin{aligned} C_2 &= \frac{1}{4\pi^2 \times 33,000^2 \times 1.94 \times 10^{-6}} \\ C_2 &= 12.01\ \mu\text{F} \end{aligned} \tag{5}$$

An alternative design could have the resonant capacitor on the primary side of the circuit as shown in Fig. 12 [8–10]. It would allow the capacitor to be loaded with low currents from the inverter rather than high currents in the secondary. The transformer ratio would reduce to around 1:2 in order to accommodate the resonant

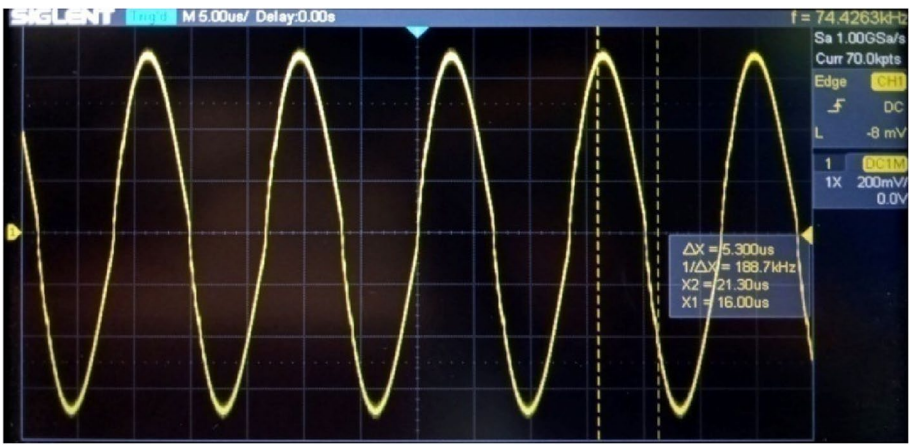

Fig. 11 Resonant current/inverter current of series resonant induction heater

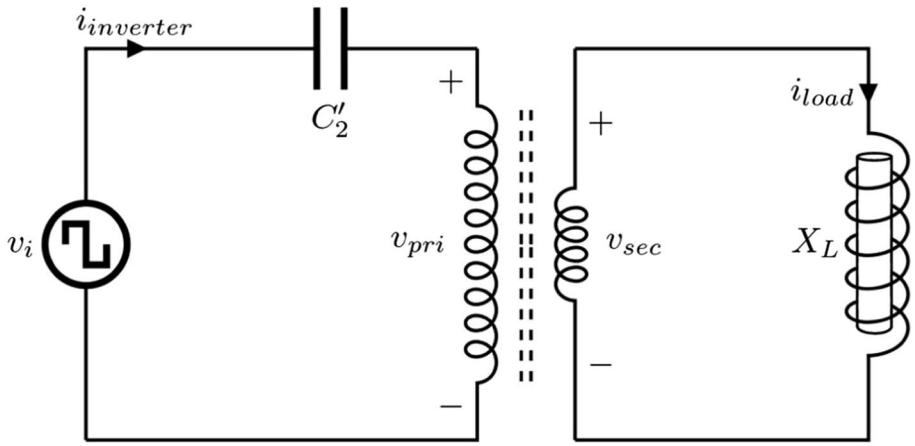

Fig. 12 Series resonant isolated heating circuit with primary side resonant capacitor

voltages. The capacitor would be subjected to higher resonant voltages as many times as the transformer ratio [6].

With the transformer ratio as 1:12, the value of capacitance required on the primary side for the same resonant frequency is calculated as [15]

$$C'_2 = \frac{C_2}{k^2} \tag{6}$$

where, k is the transformer ratio = 12.

Substituting the value of C_2 from (2),

$$C'_2 = \frac{12.01\times10^{-6}}{12^2}$$

$$C'_2 = \ 83.33nF$$

Impedance matching transformer

The impedance matching transformer primarily helps in matching the voltage and current levels of the inverter side and load side. The transformer ratio depends on the type of resonant circuit and other parameters. Ferrite with high core resistance and the ability to handle flux densities up to 1500 Guass was found suitable as the core material for the transformer. Other types of cores such as sendust and iron powder cores, even though capable of handling higher flux densities up to 10,000 to 15,000 Guass, produce a high amount of heat due to core losses. Minimum number of primary turns considering the fundamental component primary winding of the transformer is calculated using its emf equation, to prevent saturation of the transformer core during circuit operation [16].

$$N_{pri} = \frac{V_{dc} \times 10^8}{4 \times f \times B_{max} \times A_c} \tag{7}$$

where V_{dc} is the DC link voltage (V)

f is the inverter frequency (Hz)

$B_{\max}$ is the maximum flux density (*Guass*) and
A_c is the area of the magnetic core (cm^2).

$$N_{pri} = \frac{325 \times 10^8}{4 \times 33 \times 10^3 \times 1300 \times 15.6}$$

$$N_{pri} = 12.14$$

Driver power supply isolation

The driver circuit for the IGBTs would normally require a separate power supply as in this application. It would seem convenient to use a switch mode power supply (SMPS). However, it is extremely important to note that these SMPS modules have Class-Y safety capacitors (few nano-farad) linking the AC power supply side to the output for suppressing electromagnetic interference. With the SMPS connected as a power supply to the IGBT driver circuits, a weak capacitive link is formed between any one of the AC supply terminals and the DC link as shown with the capacitor C_s in Fig. 13, resulting in the malfunction of the controller due to high-frequency switching noise from the IGBTs.

At no load or lightly loaded conditions, the capacitor C_s charges up the DC link voltage up to twice the peak value of the AC supply voltage, which would damage the driver ICs and the IGBTs if they are not rated for such high voltages. For 230 V AC supply voltage, the overvoltage on the DC link could reach over 600 V as shown in Fig. 14.

The overvoltage issue can be overcome by using truly isolated power supplies or transformer-based rectifier circuits as power supply for the IGBT driver circuits.

Heating power control

Power control in a series resonant induction heater could be achieved in various ways. Controlling the AC input to the rectifier, using a controlled rectifier, and controlling the inverter output through PWM (pulse width modulation) are obvious ways. While the first two methods are does not have any undesirable effect, PWM moves the control

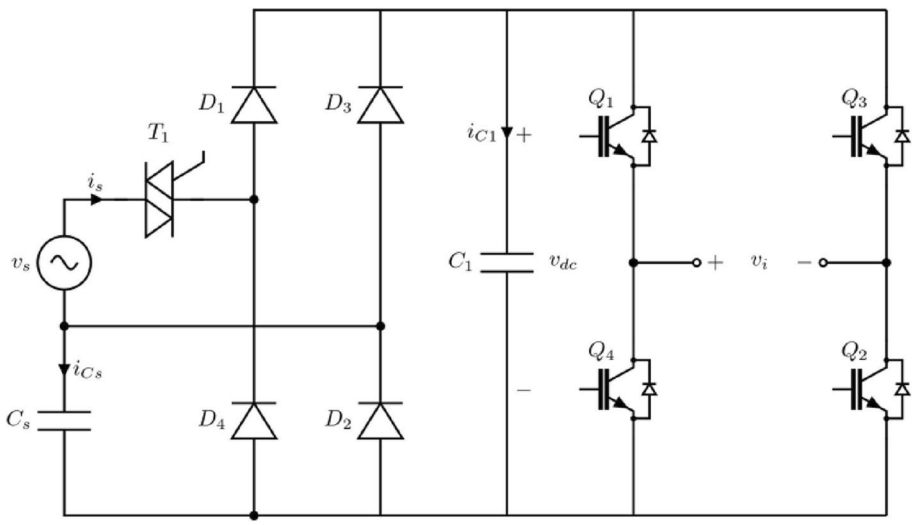

Fig. 13 Power circuit showing the equivalent of Class-Y safety capacitor appearing between the AC supply and the DC link

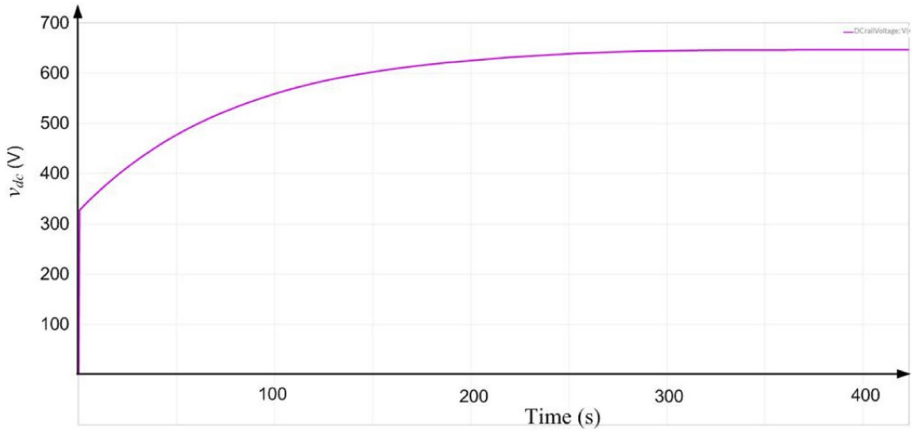

Fig. 14 Graph showing over voltage issue due to capacitive coupling between the AC source and the DC link

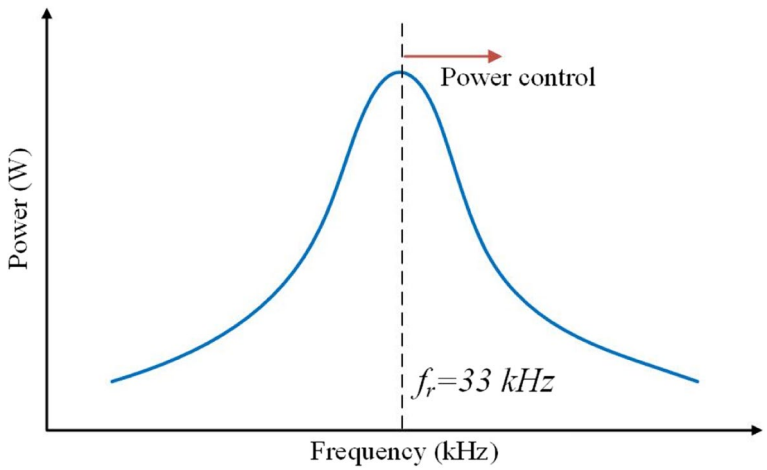

Fig. 15 Power–frequency curve of series resonant induction heater showing the region of power control

away from resonant switching and causes a significant increase in switching losses even at low power levels [7, 11].

Power control can also be accomplished by changing the transformer ratio. However, this method could not be adopted to control power during the circuit operation.

Another interesting method of controlling power is to adjust the operating frequency of the inverter with respect to the resonant frequency as shown in Fig. 15 [15, 17]. The power output reduces when the inverter frequency is moved away from the resonant frequency on either side. With a square wave inverter, it is important that the frequency is adjusted above resonance [17] in order to avoid high di/dt inverter currents due to the capacitive nature of the circuit below the resonant frequency that may result in failure of the switching devices.

In the given application, the inverter frequency is adjusted to 37 kHz to set the maximum power level at 3. 5 kW during operation. It should however be noted that due to the inverter operation slightly deviating from resonance, there would be an increase in switching losses [11], accompanied with a reduction in conduction losses due to

lower inverter currents, making the overall increase in the heat produced by the IGBTs insignificant.

Results and discussion

System implementation and experimental findings

The system is implemented in the operational environment of the servo valve test setup as per the block diagram shown in Fig. 2. The power circuit with AC voltage controller, diode bridge rectifier, and water-cooled IGBT inverter with polyester DC link capacitors is shown in Fig. 16. The controller is isolated from the driver and power circuit through high-speed opto-couplers to ensure safety with resulting IGBT gate pulses as shown in Fig. 17. The charging and discharging behaviors of the gate capacitance of the IGBTs, and the 2. 5 μs dead time could also be observed. An alternative design of the IGBT driver circuit was experimented with pulse transformers to provide isolated gate pulses for multiple IGBT, but was not considered for the implementation due to severe distortions observed in the gate pulses due to inductive coupling, which could be seen in Fig. 18.

Figure 19 shows the power circuits with the accessories such as auxiliary power supplies and the cooling system for IGBTs and the heating coil. The high-frequency transformer should preferably be placed as close as possible to the inverter output to avoid stray inductance of the cables affecting the performance of the circuit. A pair of twisted cables is used for an unavoidable distance of 2 m between the inverter output and the transformer, as both couldn't be brought any closer. Twisted cables help break large inductance loops into smaller ones and bring bipolar currents close to each other to help reduce the effect of stray inductances.

The impedance matching transformer, capacitor bank, and heating coil are arranged as shown in Fig. 20. The heating coil and the secondary winding of the transformer

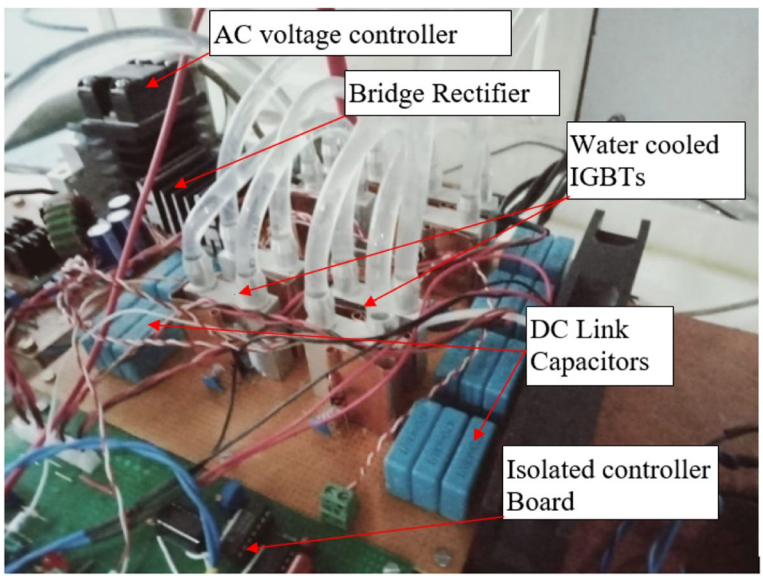

Fig. 16 Power circuit of the induction heating system showing the AC voltage controller, rectifier, and the IGBT inverter

Fig. 17 IGBT Gate pulses obtained from driver circuit based on high-speed opto-coupler

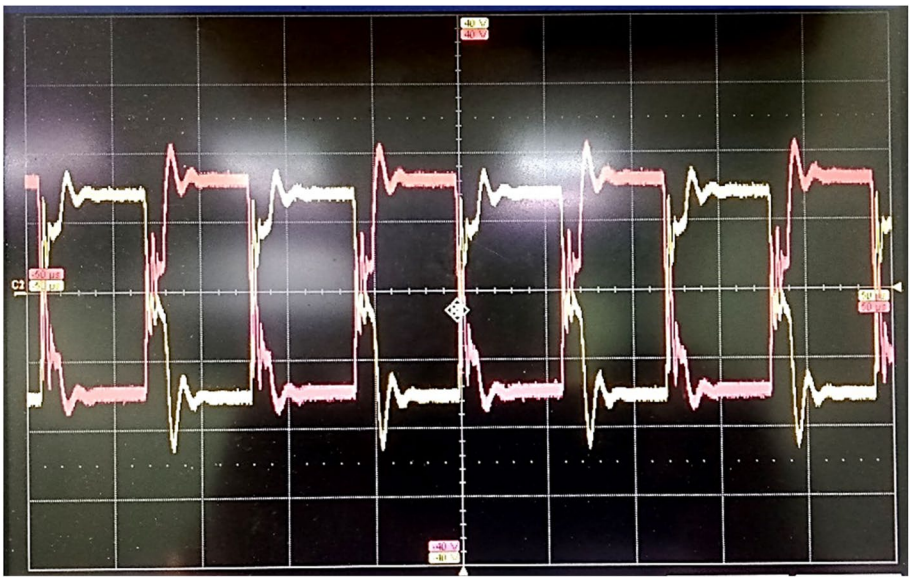

Fig. 18 IGBT Gate pulses obtained from pulse-transformer-based driver circuit

are water cooled to help the removal of heat produced by the large magnitudes of the resonant currents in the secondary circuit. The 12 μF capacitor bank is realized with individual 1 μF high current polyester 1 μF capacitors connected in parallel. In this case, the individual capacitors could be connected in series to obtain the capacitance of 83. 33 nF and connected in the primary side of the circuit for the same resonant frequency. It should be noted that the one-to-one relationship of capacitance values between parallel series connections is because of the transformer ratio is 1:12.

The arrangement of the inductive heating coil in the servo valve test setup can be seen in Fig. 21. Electrical isolation due to impedance matching transformer proves

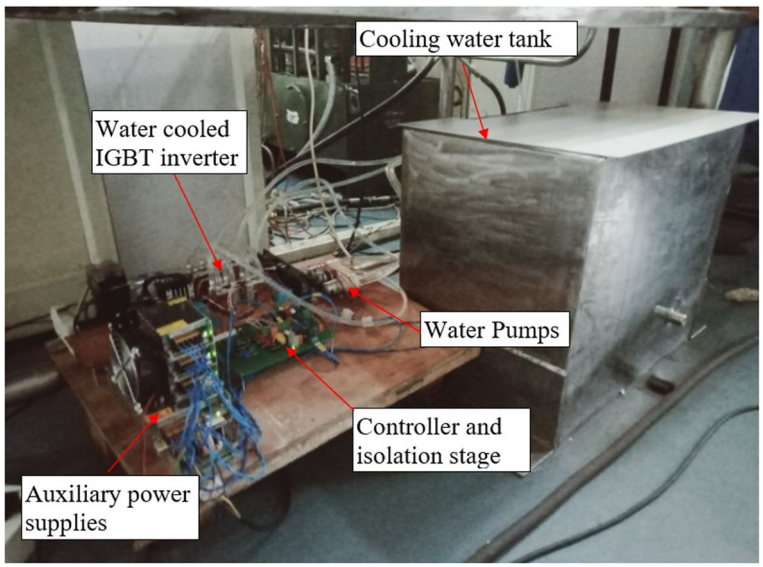

Fig. 19 Power circuit of the induction heating system with accessories

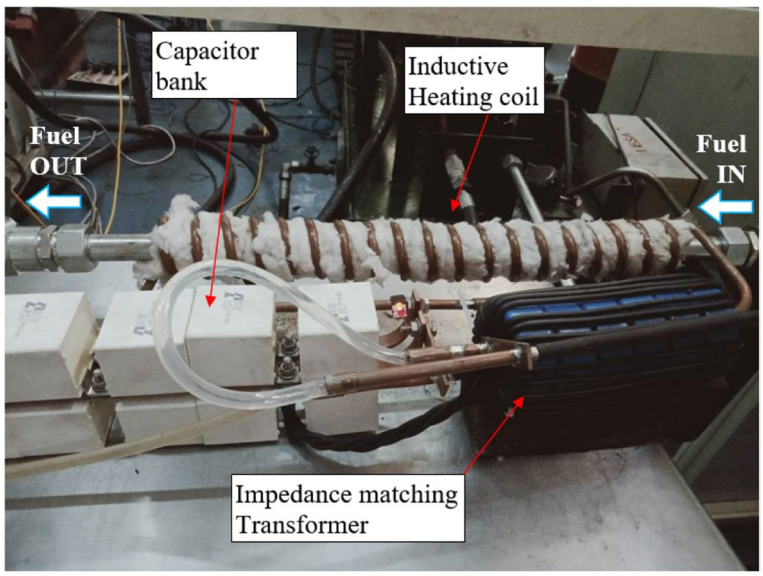

Fig. 20 Heating circuit with inductive heating coil, capacitor bank, and the impedance matching transformer

induction heating to be much safer than resistive heating in addition to the other benefits such as isolation from high pressure and clean heating.

The actual temperature profile of hours 176 to 180 out of 300 continuous hours of servo valve testing is shown in Fig. 22 and that of hours 293 to 300 is shown in Fig. 23. The 10-min temperature ramp from 45 °C to 90 °C, 90 °C to 45 °C and the steady temperature level of 90 °C for 35 min are achieved as per the desired temperature profile.

The induction heater handled the desired power rating of 4 kW with low heat losses due to the near-resonant switching. Smooth control of temperature is achieved due to the efficient operation of the induction heating system with closed-loop control. A highly reliable heating arrangement for the high-pressure testing application

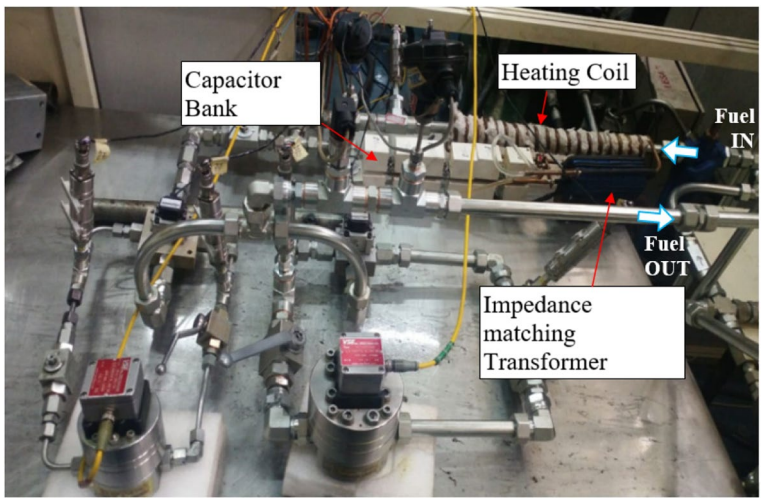

Fig. 21 Servo valve test setup with induction heating arrangement

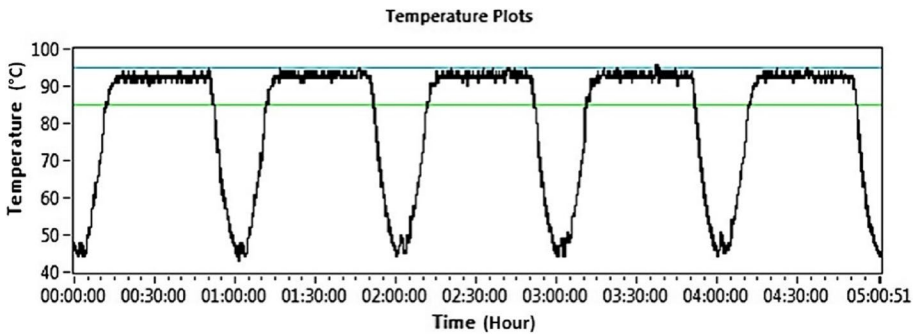

Fig. 22 Actual temperature profile during hours 176 to 180 of the servo valve test

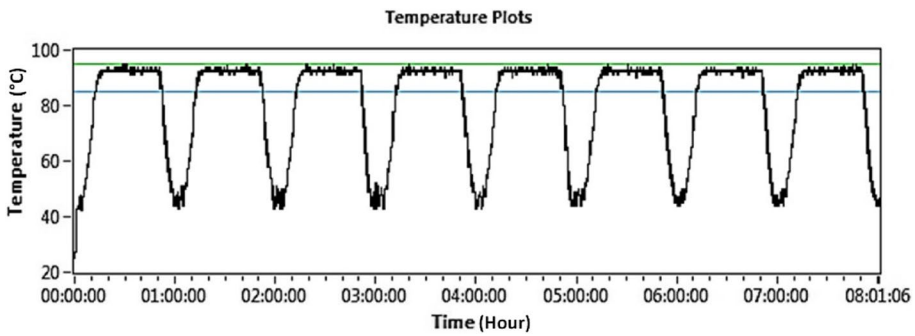

Fig. 23 Actual temperature profile during hours 293 to 300 of the servo valve test

at 84 bar with inline heated fuel is developed based on a clear understanding of the functional differences between the various configurations of the induction heating system and the challenges in designing the individual component of the system.

Efficiency analysis

The efficiency analysis of the induction heating system helps us determine how effectively the system converts electrical energy into heat and how efficiently it transfers that heat to the target substance, in this case, the aviation fuel. Various factors influence the overall efficiency of the induction heating system, such as the design of the resonant tank circuit, the selection and operation of the IGBT inverter, and the cooling arrangements for the power components. Additionally, the impedance matching transformer and capacitor bank configuration can impact the energy transfer efficiency. By carefully analyzing these factors and quantifying the losses incurred at different stages of the heating process, we can gain insights into the system's energy efficiency and identify areas for improvement. The efficiency analysis provides insights into the magnitude of power losses occurring in various components of the system, including the power circuit, driver circuit, and auxiliary components like the ferrite core transformer, heating coils, and cables.

Extensive simulations were carried out in LTspice to assess the power losses occurring in the various components of the power conversion circuits. The power electronic converter exhibited efficiencies between 94 to 96% in the simulations. Most of the power losses are attributed to the switching losses and conduction losses in high-frequency electronic switching devices and the conduction losses in the bridge rectifier. However, the actual system exhibited additional power loss in the distributed resistance of the electrical cables and due to heat radiation near the outer surface of the workpiece through its insulation layer of glass wool. These observations were further validated through experimental measurements of efficiency.

The output power that is transferred to the fuel as heat is calculated as [18]

$$P_{out} = d \times q \times C \times \Delta T \tag{8}$$

where d is the density of the Jet A1 fuel (840 kg/m^3),
q is the flow rate of the fuel inside the heating pipe (1 lpm = 16.667×10^{-6} m^3/s),
C is the specific heat of the fuel (2.2 kJ/kg°K), and
ΔT is the difference in temperature after and before heating (90–45 °C = 45 °C).

$$P_{out} = 840 \times 2.2 \times 10^3 \times 16.667 \times 10^{-6} \times 45$$

$$P_{out} = 1.386\,\text{kW}$$

The input power to the induction heating system is given by

$$P_{in} = k \times V_{rms} \times I_{rms} \tag{9}$$

where k is the duty ratio of the AC voltage controller,
V_{rms} is the rms value of input voltage (V), and
I_{rms} is the rms value of input current (A).

$$P_{in} = 0.45 \times 230 \times 14.6$$
$$P_{in} = 1.511\,\text{kW}$$

The efficiency of the induction heating system is given by

$$\begin{aligned} \eta &= \frac{P_{out}}{P_{in}} \\ \eta &= \frac{1.386}{1.511} \\ \eta &= 0.917 \text{ or } 91.7\% \end{aligned} \tag{10}$$

Based on the calculated efficiency of 91.7% for the heating system, it is evident that there is a drop in efficiency compared to the power electronic converter's efficiency of 94 to 96%. This decrease in efficiency can be attributed to various factors, including heat radiation from the fuel pipe, which results in heat loss rather than efficient heat transfer to the fuel. However, it should be noted that these efficiency values are much higher than the practical efficiencies of other heat exchanger-based systems which lie around 60–70% or even less. Further analysis and optimization efforts can focus on mitigating heat losses and improving heat transfer mechanisms to achieve higher efficiencies in future iterations of the induction heating system.

Comparison with alternative designs

In comparison to the commonly used high-pressure heat exchanger-based system for fuel heating, our proposed inline induction heating system offers several significant advantages. The high-pressure heat exchanger-based system utilizes thermic fluid and water for heating and cooling the fuel, respectively, resulting in energy losses due to large thermal inertia, increased complexity, and higher costs. Dedicated systems are required for heating the thermic fluid and cooling the water in a heat exchanger-based system, which makes the system much more complex. Moreover, high-pressure heat exchangers are typically made of steel, which exhibits poorer heat transfer response compared to low-pressure aluminum heat exchangers. The system also requires the use of flow control valves for the thermic fluid and cooling water, further contributing to its complexity and cost.

In contrast, our inline induction heating system provides localized heating, rapid response, efficient cooling due to low-volume heating, fewer heat transfer components, precise control, and overall cost savings. The design cost of our inline induction heating system was approximately ₹ 15,000, significantly lower than the estimated cost of approximately ₹ 10 lakh for the heat exchanger-based system.

Commercially available induction heating systems have been widely used for various applications. These systems employ induction heating as the primary mechanism, providing efficient and controlled heating. However, when it comes to high-pressure inline heating, these off-the-shelf systems may not be suitable without certain modifications. Typically, these systems require adjustments to the resonant components and the incorporation of closed-loop control to meet the specific requirements of inline heating. Additionally, the control capabilities of these systems are often limited, relying on manual control options. Incorporating automatic control may necessitate further modifications. Despite their moderate energy efficiency, these commercially available systems lack optimization for specific applications, resulting in moderate material efficiency. The

complexity of repurposing these systems for high-pressure inline heating is also a factor to consider. Moreover, the cost of such systems tends to be high, ranging from ₹ 3–5 lakh, and their maintenance can incur significant service costs. Safety is another concern, as the heating coils may not be isolated from the mains, and the system behavior may be unpredictable.

The following table provides a comprehensive comparison between our proposed inline induction heating system, the heat exchanger-based system, and commercial induction heating systems, highlighting their key attributes and performance parameters (Table 1).

The comparison between our proposed inline induction heating system, the heat exchanger-based system, and commercial induction heating systems reveals distinct advantages of our proposed solution for high-pressure fuel heating applications. The inline induction heating system offers localized heating, almost instantaneous response, precise control, high energy and material efficiency, low complexity, cost-effectiveness, minimal maintenance requirements, and enhanced safety measures. In contrast, the heat exchanger-based system exhibits limitations in terms of slower response, increased energy losses, higher complexity, and maintenance demands. Commercial induction heating systems, while not readily available for high-pressure inline heating, require modifications and lack customization options. Based on these findings, our proposed inline induction heating system emerges as a superior choice, offering a compelling alternative for high-pressure fuel heating applications with its exceptional performance, efficiency, and cost-effectiveness.

Conclusions

The present study aimed to develop an efficient and reliable induction heating system for high-pressure fuel heating applications. Extensive research was conducted on various configurations of induction heater circuits, considering factors such as power efficiency, system complexity, and heat transfer mechanisms. Based on this analysis, the high-pressure fuel inline heating system with a series resonant induction heater with isolation using an impedance matching transformer was selected as the most suitable configuration.

The proposed induction heating system offers several distinct advantages over alternative designs, particularly the commonly used high-pressure heat exchanger-based system. By utilizing localized heating and precise control, our system provides almost instantaneous response and high energy efficiency. Furthermore, the design cost of the proposed inline induction heating system is significantly lower than that of the heat exchanger-based system, making it a cost-effective solution for high-pressure fuel heating.

This study provides a comprehensive analysis of induction heater circuits, considering various factors such as power conversion efficiency, impedance matching, and driver power supply isolation. The findings not only contribute to the understanding of different configurations but also provide practical insights for designing efficient and reliable induction heating systems for specific applications.

Table 1 Proposed induction heating system vs. heat exchanger-based system

Aspect	Proposed inline induction heating system	Heat exchanger-based system	Commercial induction heating system
Heating mechanism	Induction heating, offering localized heating, almost instantaneous response, and precise control for high-pressure in-line heating of fuel.	Heat exchangers, those rely on thermic fluid and water for heating, leading to higher thermal inertia and slower response.	Induction heating, with systems not suitable for high-pressure inline heating, requiring modifications to the resonant components and incorporating closed-loop control.
Control capabilities	Precise, with almost instantaneous response.	Limited, with slow response due to large thermal inertia.	Limited, due to manual control options. Incorporating automatic control would require modifications.
Energy efficiency	High, due to direct energy transfer, localized heating, resulting in minimal energy losses and careful selection of components.	Low, with increased energy losses due multiple heat transfer components, limited options for optimization, and wastage of energy for cooling.	Moderate, due to their generic design and lack of optimization for specific applications.
Material efficiency	Good, as the proposed system requires fewer heat transfer components, minimizing material usage and potential points of failure.	Poor, as heat exchanger-based systems use multiple heat transfer components, liquid storage elements, and its associated control components, increasing material requirements and maintenance needs.	Moderate, as the system might be oversized and would lack customization options.
Complexity	Low, due to one heat transfer component and self-contained power converter with closed-loop control.	High, due to the complexity of integrating multiple components such as heat exchangers, flow control systems, thermic fluid heating system, water cooling system, and safety requirements into a cohesive system.	Moderate, due to the modifications required for purposing the commercial induction heating system into a high-pressure inline heating setup.
Cost	Low, with a design cost of approximately ₹ 15,000.	Highly expensive, estimated to cost around ₹ 10 lakh.	High, with prices around ₹ 3–5 lakh.
Maintenance	Minimum and Easy, as the heat transfer component is just a steel pipe.	Maximum, as many components such as heat exchangers, flow control valves, heating system, and cooling system are involved.	Moderate, as the service costs would be high.
Safety	Most safe, as the system is electrically isolated from mains and uses safe length of the heating pipe with temperature protection.	Less safe, due to the potential risks of leaks, spills, and accidents associated with heat exchangers, other components, and joints.	Less safe, as the heating coils may not be isolated from the mains and the behavior of the system could be unpredictable.

The developed induction heating system demonstrates exceptional performance, energy efficiency, and cost-effectiveness, making it a compelling alternative for high-pressure fuel heating applications. This research contributes valuable knowledge on induction heater circuits and provides a practical solution for high-pressure fuel heating. The findings pave the way for further optimization and future advancements in induction heating technology, ultimately benefiting industries that require efficient and reliable heating processes.

Abbreviations

LRU	Line replacement unit
lpm	Litre per minute
PID	Proportional integral derivative
AC	Alternating current
DC	Direct current
IGBT	Insulated gate bipolar transistor
PWM	Pulse width modulation

Acknowledgements
This research and development work is financially supported by Central Manufacturing Technology Institute, Bengaluru, Karnataka, India.

Authors' contributions
TT conceived the idea of inline induction heating of high-pressure fuel, devised the process control, and analyzed the thermal characteristics, and material properties; EGR designed and developed the induction heater circuits, implemented closed-loop control, and contributed to the writing of the manuscript; MM analyzed the flow and heat transfer; NS implemented the hydraulic system for the testing arrangement. All authors have read and approved the manuscript.

Funding
This research work was internally funded by CMTI-Bengaluru, India.

Availability of data and materials
Not applicable.

Declarations

Competing interests
The authors declare that they have no competing interests.

Received: 30 March 2023 Accepted: 20 July 2023
Published online: 28 September 2023

References

1. Kamli M, Yamamoto S, Abe M (1996) A 50–150 kHz half-bridge inverter for induction heating applications. IEEE Trans on Ind Elec 43(1):163–172. https://doi.org/10.1109/41.481422
2. Calleja H, Ordonez R (1999) Induction heating inverter with active power factor correction. Int J of Elec 86(9):1113–1121. https://doi.org/10.1080/002072199132888
3. Lucia O, Maussion P, Dede EJ, Burdio JM (2014) Induction heating technology and its applications: past developments, current technology, and future challenges. IEEE Trans Ind Elec 61(5):2509–2520. https://doi.org/10.1109/TIE.2013.2281162
4. Park HS, Dang XP (2012) Optimization of the in-line induction heating process for hot forging in terms of saving operating energy. Int J Precis Eng Manuf 13(7):1085–1093. https://doi.org/10.1007/s12541-012-0142-z
5. Lucia O, Acero J, Carretero C, Burdio JM (2013) Induction heating appliances: toward more flexible cooking surfaces. IEEE Ind Elec Mag 7(3):35–47. https://doi.org/10.1109/MIE.2013.2247795
6. Andrew A, Jih-S L (2015) A transformer-coupled, series-resonant topology for the induction heating of aluminum cookware. 9th Int. C. on Power Elec., ECCE-Asia (ICPE-ECCE Asia). https://doi.org/10.1109/icpe.2015.7167938
7. Vishnuram P, Ramachandiran G, SudhakarBabu T, Nastasi B (2021) Induction heating in domestic cooking and industrial melting applications: a systematic review on modelling converter topologies and control schemes. Energies 14(20):6634. https://doi.org/10.3390/en14206634
8. Oncu S, Unal K, Tuncer U (2022) Laboratory setup for teaching resonant converters and induction heating. Eng Sci Tech Int J. https://doi.org/10.1016/j.jestch.2021.05.016
9. Iagăr A, Popa GN, Diniş CM (2015) Analysis the electrical parameters of a high-frequency coreless induction furnace. IOP Conf Ser: Mater Sci Eng. https://doi.org/10.1088/1757-899X/85/1/012013

10. Karafil A, Ozbay H, Oncu S (2021) Comparison of regular and irregular 32 pulse density modulation patterns for induction heating. IET Power Elec 14:78–89. https://doi.org/10.1049/pel2.12012
11. Hu J, Bi C, Jia K, Xiang Y (2015) Power control of asymmetric frequency modulation in full-bridge series resonant inverter. IEEE Trans Power Elec. 1(1). https://doi.org/10.1109/tpel.2014.2384523
12. Kim JW, Lee M, Lai JS (2018) A new control method for series resonant inverter with inherently phase-locked coil current with induction cookware applications. IEEE Applied Power Elec Conf Expo. (APEC) - San Antonio. 3517–3522. https://doi.org/10.1109/APEC.2018.8341611
13. Llorente S, Monterde F, Burdio JM, Acero J (2002) A comparative study of resonant inverter topologies used in induction cookers. IEEE APEC - Applied Power Elec Conf Expo. - Dallas, TX, USA :2(0):1168–1174. https://doi.org/10.1109/apec.2002.989392
14. Indhuja LR, Christy Mano Raj JS (2022) Design and development of voltage fed series resonant inverter for induction heating applications. Int J Creat Res Thoughts (IJCRT) 10(6):605–615
15. Tan X, Ruan X (2015) Equivalence relations of resonant tanks: a new perspective for selection and design of resonant converters. IEEE Trans Ind Elec. 1(1). https://doi.org/10.1109/TIE.2015.2506151
16. Bi C, Lu H, Jia K, Hu J, Li H (2016) A novel multiple-frequency resonant inverter for induction heating applications. IEEE Trans Power Elec. 1(1). https://doi.org/10.1109/TPEL.2016.2521401
17. Park SM, Jang E, Joo D, Lee BK (2002) Power curve-fitting control method with temperature compensation and fast-response for all-metal domestic induction heating systems. Energies 12(15):1–16. https://doi.org/10.3390/en12152915
18. Kilic VT, Unal E, VolkanDemir H (2020) High-efficiency flow-through induction heating. IET Power Electronics 13(10):2119–2126. https://doi.org/10.1049/iet-pel.2019.1609

Publisher's Note

Tom Thampy Tom Thampy is currently working as Scientist-D at the Central Manufacturing Technology Institute in Bengaluru. He has a broad experience in the design and development of test rigs for qualifying pneumatic, hydraulic, and electrohydraulic airworthy LRUs. He has contributed his expertise to various technical projects such as development of electro-hydraulic pneumatic separators, battery-operated hydraulic rigs, modal analysis of machine tool structures, and endurance testing of hydraulic elements. Additionally, Tom has published technical papers on topics such as pressure impulse testing, electro-hydraulic force excitation, optimization of flow control valves using recursive methods, etc. His outstanding contributions have been recognized through awards like the IEI Young Engineers Award and the MEDIC Innovation Award.

Emmanuel Gospel Raj Rivington Emmanuel Gospel Raj Rivington is currently working as Project Fellow in Central Manufacturing Technology Institute, Bengaluru. His areas of interest include power electronics, control engineering, system development, microcontrollers, etc. He has experience in the design and development of high-power, high-frequency electronic circuits, control systems, and other innovative applications. Emmanuel has successfully contributed to a wide range of projects, including the development of solenoid valves, induction heating systems, UVC disinfection devices, image processing systems, and instrumentation amplifiers. He was previously a faculty member where he had handled many lectures on electrical engineering, microcontrollers, power electronics, and electrical drives. Emmanuel has contributed to the field of engineering through his research publications on diverse topics such as speed measurement, optimization of flow control valves, smart technology applications, robotics, and energy management. He has received several awards and recognitions for his innovative ideas and technological contributions.

Madan Mohan Avulapati Madan Mohan Avulapati is currently working as an Assistant Professor in the Department of Mechanical Engineering at the Indian Institute of Technology Tirupati. His research interests encompass a wide range of areas including liquid atomization, combustion, alternative fuels for internal combustion engines and gas turbines, as well as optical diagnostics for spray, combustion, and multiphase flows. With a wealth of experience in industry, research, and teaching, Madan Mohan has made significant contributions to the fields related to engines, combustion, materials, and fluid mechanics. He has authored several notable publications, including research papers on topics such as liquid sheet breakup, secondary breakup of water and surrogate fuels, spray evolution and ignition in high-pressure spray flames, biofuels and spray interactions, and the dynamics of micro-explosion and puffing in emulsion droplets. His research findings provide valuable insights into atomization processes,

fuel combustion, and droplet dynamics, contributing to advancements in the field of energy and propulsion systems.

Niroop Srinivasa Murthy Niroop Srinivasa Murthy is currently working as Project Fellow in Central Manufacturing Technology Institute, Bengaluru. His areas of interest include Mechanical Hydraulic and Thermal designing. He is involved in the design and development of test rigs and test fixtures. He is involved in the characterization of inline heating for high-flow fluids with respect to input power done CFD analysis for different hydraulic components. He is involved in Vibration analysis of the electro-hydraulic Actuator's vibration test fixtures. Designing of hydraulic circuits for testing at high and subzero temperatures.